Tracking unstable periodic orbits in a bronze ribbon experiment

U. Dressler, T. Ritz, and A. Schenck zu Schweinsberg
Daimler-Benz AG, Research Institute Frankfurt, Goldsteinstrasse 235, D-60528 Frankfurt, Germany

R. Doerner, B. Hübinger, and W. Martienssen
Physikalisches Institut der Johann Wolfgang Goethe-Universität, Robert-Mayer-Strasse 2-4, D-60325 Frankfurt am Main, Germany

(Received 16 September 1994)

We demonstrate the tracking of an unstable periodic orbit (UPO) in a bronze ribbon experiment. The stabilization of the UPO at each tracking step is performed via the local control method, a variant of the Ott-Grebogi-Yorke [Phys. Rev. Lett. **64**, 1196 (1990)] feedback control method. Starting with feedback control vectors extracted from the analysis of the experimental data at each tracking step, we redetermine the location of the UPO using an adaptive orbit correction that exploits the applied control signal and the actual trajectory of the system. Doing so, the unstable periodic orbit can be tracked into a parameter regime where the chaotic attractor has long ago lost its stability and another periodic orbit has become stable.

PACS number(s): 05.45.+b

INTRODUCTION

The control idea of Ott, Grebogi, and Yorke (OGY) to stabilize unstable periodic orbits (UPOs) embedded in a chaotic attractor by feedback control [1] has triggered immense research activity to apply feedback control to chaotic systems (see [2] and references therein). An immediate and most promising extension of OGY's control method is the tracking idea of Schwartz and Triandaf [3]. They propose to first stabilize an UPO lying in a chaotic attractor and then to slowly alter the control parameter p while adjusting the control values of the feedback loop to its new actual values such that control is maintained over the whole tracking process. The tracking idea in combination with OGY's control method has direct impact on the possibility of real world applications of this type of chaos control. Having a reliable tracking method at hand, one can deal with fluctuating external parameters, which improves the stability of OGY's control for technical systems, and furthermore it is possible to extend the range of stability of a system [4]. The feasibility of the tracking idea has been demonstrated experimentally in an electronic circuit [5], in a laser experiment [4], and in the Belousov-Zhabotinsky reaction [6]. A slightly different tracking technique, which does not need parameter adjustment over a whole parameter regime, is reported in a laser experiment in [7].

While all these experiments [4–6] follow the same tracking idea, they differ in two aspects: First, in the variant of OGY's feedback control method, which is applied for control (original OGY [5], occasional proportional feedback [8,4], a map based algorithm [6]), and second, in details of the strategy used to determine the correct parameters of the feedback loop for each new tracking step.

To explain the main ingredients of a tracking strategy let us briefly recall the fundamental equation of OGY's feedback control for a two-dimensional map $\mathbf{z}_{n+1} = \mathbf{P}(\mathbf{z}_n, p + \delta p_n)$. To stabilize an unstable fixed point $\mathbf{z}_F(p) = \mathbf{P}(\mathbf{z}_F(p), p)$ by small parameter perturbations δp_n around p, one uses the fact that in the neighborhood of $\mathbf{z}_F(p)$ the dynamics can be described by the linearization of $\mathbf{P}$ around $\mathbf{z}_F(p)$ and p, i.e.,

$$\delta\mathbf{z}_{n+1} \approx A(p)\delta\mathbf{z}_n + \mathbf{w}(p)\delta p_n \tag{1}$$

with $\delta\mathbf{z}_n = \mathbf{z}_n - \mathbf{z}_F(p)$, $\delta p_n = p_n - p$, $A(p) = D_{\mathbf{z}}\mathbf{P}(\mathbf{z}_F(p), p)$, and $\mathbf{w}(p) = \frac{\partial \mathbf{P}(\mathbf{z}_F(p),p)}{\partial p}$. Requiring as a stability condition that the next state $\mathbf{z}_{n+1}$ shall fall on the stable direction of the fixed point the linearization leads to the feedback condition [1]

$$\delta p_n = \mathbf{K}(p) \cdot (\mathbf{z}_n - \mathbf{z}_F(p)) \ , \tag{2}$$

which is applied only when the magnitude of δp_n is less than a maximal allowed parameter perturbation $\delta p_{\max}$. The two-dimensional control vector $\mathbf{K}(p)$ [which is calculated using $A(p)$ and $\mathbf{w}(p)$] and the position of the UPO $\mathbf{z}_F(p)$ are the parameters of the feedback loop of the OGY control.

While a small deviation of the control vector $\mathbf{K}(p)$ from its optimal value influences primarily the time one needs for successful control [9], an error in the determination of $\mathbf{z}_F(p)$ results in a systematic deviation of the averaged control signal $\langle \delta p_n \rangle$ from zero [3], which is proportional to the difference between the true fixed point $\hat{\mathbf{z}}_F(p)$ and the reference fixed point $\mathbf{z}_F(p)$ used in the feedback loop (2):

$$|\langle \delta p_n \rangle| \propto \|\mathbf{z}_F(p) - \hat{\mathbf{z}}_F(p)\|. \tag{3}$$

It is this relation that Schwartz and Triandaf exploit

in their tracking procedure [3] in order to correct a prediction of $\hat{\mathbf{z}}_F(p)$. At each tracking step they vary the reference value $\mathbf{z}_F(p)$ in the feedback loop until the averaged control signal $|\langle \delta p_n \rangle|$ is minimized.

In the tracking experiment we present in this paper, we use the adaptive orbit correction recently introduced by Doerner *et al.* [10] in order to redetermine the position of $\mathbf{z}_F(p)$ at each tracking step. For a one-dimensional map this approach coincides with the orbit correction used by Petrov *et al.* in [6]. The adaptive orbit correction allows one to calculate a new estimate of $\hat{\mathbf{z}}_F(p)$ using an explicit relation between the control signal, the actual controlled trajectory, and the true UPO $\hat{\mathbf{z}}_F(p)$. The feasibility of this approach is demonstrated for a vibrating bronze ribbon. In [11] we reported how to control this experiment for a specific parameter value with the local control method of Hübinger *et al.* [12], a variant of OGY's feedback control. We now report successful tracking of an UPO from that parameter value into a parameter regime where the chaotic attractor has long ago lost its stability.

THE BRONZE RIBBON EXPERIMENT

The experimental setup was stimulated by the magnetoelastic beam experiment of Moon [13]. It is described in detail in [11], so that we now only briefly sketch some important features.

The experiment is a horizontally cantilevered elastic bronze ribbon which is periodically driven (see the experimental setup in Fig. 1). As a measurement signal $x(t)$ we use the voltage signal which is related to the deflection of the vibrating beam. With this measurement signal the chaotic attractor is reconstructed in the embedding space $(x, \dot{x}, \theta)$, with $\dot{x}$ obtained from numerical differentiation of the signal and $\theta(t) = \frac{2\pi}{T}t$ being the phase of the periodic driving $U_A \sin\theta$. For the control parameter $p = 0$ V we find a chaotic attractor with three highly unstable period-one orbits ($|\lambda_u| \approx 10$, λ_u being the unstable eigenvalue of the UPO) [11]. This large instability prevents a successful feedback control if one uses only one control step per period of the driving, i.e., only one Poincaré section. If, however, one increases the frequency of control, which is done by the local control method, the experiment can be successfully controlled [11].

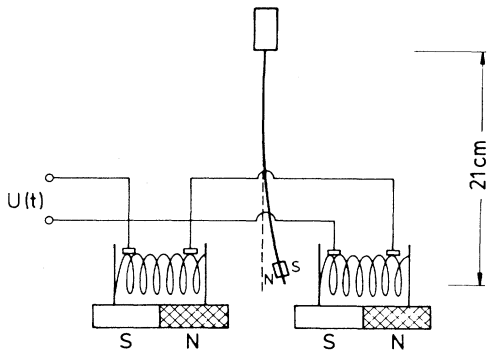

FIG. 1. Experimental setup of the chaotic bronze ribbon. A horizontally cantilevered bronze beam equipped with two small permanent magnets is located in an inhomogeneous magnetic field. Two coils are placed around the free end of the beam and are supplied with an ac voltage $U(t) = U_A \sin\frac{2\pi}{T}t + p$, $U_A = 0.6$ V, and the driving period $T = 1$ s. The offset voltage p is used as control parameter. Measurements are taken with a wire strain gauge at the fixed end of the beam to obtain a voltage signal x related to the deflection of the beam.

LOCAL CONTROL METHOD

The local control method introduces N equally spaced Poincaré sections Σ_n, $n = 1, \ldots, N$. For a periodically driven system (with driving period T) this leads to an adjustment of the control parameter every $\Delta t = T/N$ if Σ_n are the natural Poincaré sections of constant phase $\theta_n = \frac{2\pi n}{N}$ of the driving. Thus in our experiment a point $\mathbf{z}^n$ in Σ_n is given by $\mathbf{z}^n = (x(t_n), \dot{x}(t_n))$, $t_n \bmod T = (n \bmod N)\Delta t$. Let $\mathbf{z}_F^n$ and $\mathbf{z}^n$ be the intersection of the UPO and the actual trajectory with Σ_n and $p^n = p + \delta p^n$ the valid control parameter when the system goes from Σ_n to Σ_{n+1}. The linearization around $\mathbf{z}_F^n$ and p in Σ_n of the flow map $\phi_{\Sigma_n}^{\Delta t}$, which maps a state from Σ_n to Σ_{n+1}, is given by

$$\delta \mathbf{z}^{n+1} = A^n(p)\delta \mathbf{z}^n + \mathbf{w}^n(p)\delta p^n \tag{4}$$

with $\delta \mathbf{z}^n = \mathbf{z}^n - \mathbf{z}_F^n(p) \in \Sigma_n$, $A^n = D_{\mathbf{z}_F^n}\phi_{\Sigma_n}^{\Delta t}$, and $\mathbf{w}^n = \frac{\partial \phi_{\Sigma_n}^{\Delta t}}{\delta p}$. To stabilize $\mathbf{z}_F^n$ the singular value decomposition of A^n is exploited to obtain the feedback formula

$$\delta p^n = (1 - \rho - \mu_u^n)\frac{\mathbf{v}_u^{n\dagger}\delta \mathbf{z}^n}{\mathbf{v}_u^{n\dagger}\mathbf{w}^n} \tag{5}$$

with $\rho \in (0,1)$, μ_u^n being the largest singular value of $A^n = U^n W^n V^{n\dagger}$, and $\mathbf{v}_u^n$ the corresponding row vector of V^n. For abbreviation we write (5) as

$$\delta p^n = \mathbf{K}^n(p) \cdot (\mathbf{z}^n - \mathbf{z}_F^n(p)). \tag{6}$$

So the control values for the feedback of the local control are $\mathbf{z}_F^n(p)$ and $\mathbf{K}^n(p)$, $n = 1, \ldots, N$.

ORBIT CORRECTION FROM THE CONTROL SIGNAL

As was already pointed out before, for successful tracking it is crucial to reduce a possible difference between the true unstable orbit $\hat{\mathbf{z}}_F^n$ and the reference value $\mathbf{z}_F^n(p)$ of the feedback loop (6). The correction is based on the following observation [10]. If there is a difference between the true UPO $\hat{\mathbf{z}}_F^n$ and the one used in the feedback (6), then the local control finally leads to an almost periodic trajectory $\mathbf{z}^n \approx \mathbf{z}^{n+N}$ and an almost periodic control signal $\delta p^n \approx \delta p^{n+N}$. As the observed trajectory $\mathbf{z}^n$ is still close to the true UPO $\hat{\mathbf{z}}_F^n$ and the parameter perturba-

tions δp^n are small, $\mathbf{z}^n$ and δp^n fulfill the linearization (4)

$$\mathbf{z}^{n+1} - \hat{\mathbf{z}}_F^{n+1} = A^n(\mathbf{z}^n - \hat{\mathbf{z}}_F^n) + \mathbf{w}^n \delta p^n, \qquad n = 1, \ldots, N. \tag{7}$$

For perfect periodicity of δp^n and $\mathbf{z}^n$ this set of equations can be solved with respect to $\hat{\mathbf{z}}_F^n$ to obtain a new estimate $\mathbf{z}_{F,\text{new}}^n$ of the true orbit $\hat{\mathbf{z}}_F^n$. In experiments there is never strict periodicity because of measurement noise. Therefore one averages δp^n and $\mathbf{z}^n$ over some, e.g., M, driving periods and inserts $\langle \mathbf{z}^n \rangle = \frac{1}{M} \sum_{i=0}^{M-1} \mathbf{z}^{n+iN}$ and $\langle \delta p^n \rangle = \frac{1}{M} \sum_{i=0}^{M-1} \delta p^{n+iN}$ instead of δp^n and $\mathbf{z}^n$ into the set of equations (7). Its solution with respect to $\hat{\mathbf{z}}_F^n$ gives a new estimate $\hat{\mathbf{z}}_{F,\text{new}}^n$ of the true unstable orbit.

In Fig. 2 the effect of this orbit correction in our experiment is shown. With $\hat{\mathbf{z}}_{F,\text{old}}^n$ we denote the unstable orbit used as reference orbit $\mathbf{z}_F^n$ in the feedback (6). We then record a sequence of the control signal δp^n and the stabilized (almost periodic) orbit $\mathbf{z}^n$ for $M = 4$ periods to calculate $\hat{\mathbf{z}}_{F,\text{new}}^n$ [see Fig. 2 (a)].

In experiments because of measurement noise and possible errors of A^n and $\mathbf{w}^n$ one cannot expect that the corrected orbit $\hat{\mathbf{z}}_{F,\text{new}}^n$ gives already the correct value of $\hat{\mathbf{z}}_F^n$. Therefore in our experiment we do not immediately replace the old value $\hat{\mathbf{z}}_{F,\text{old}}^n$ by $\hat{\mathbf{z}}_{F,\text{new}}^n$ in (6), but use a weighted average

$$\mathbf{z}_F^n(\chi) = (1-\chi)\,\mathbf{z}_{F,\text{old}}^n + \chi\,\mathbf{z}_{F,\text{new}}^n, \qquad \chi \in [0,1], \tag{8}$$

starting with $\chi = 0$ and increasing χ slowly. Depending on the average weighting factor χ, the magnitude of the necessary control signal, i.e., $\langle |\delta p^n| \rangle_n = \frac{1}{N} \sum_{n=1}^{N} |\delta p^n|$, changes. This is shown in Fig. 2(b). In the spirit of Eq. (3) we take as optimal χ the one that minimizes $\langle |\delta p^n| \rangle_n$ and thus finally obtain a new reference orbit $\mathbf{z}_F^n = \mathbf{z}_F^n(\chi_{\text{opt}})$ for the local control. In a tracking process this optimization of χ diminishes also the danger that an erroneous calculation of $\hat{\mathbf{z}}_{F,\text{new}}^n$ leads to a loss of control over the tracked orbit.

The necessary control signal $\langle |\delta p^n| \rangle_n$ can be diminished further by repeating the adaptive orbit correction. In addition we observed that the reduction of the maximal allowed parameter perturbation $\delta p_{\max}$ often leads to a decrease of the applied control signal. The orbit correction which we use in the tracking process therefore always consists of solving Eq. (7) with the averages $\langle \mathbf{z}^n \rangle$ and $\langle \delta p^n \rangle$ inserted, optimizing the weighting factor χ, reducing $\delta p_{\max}$ and repeating this process until no further decrease of the control signal can be achieved.

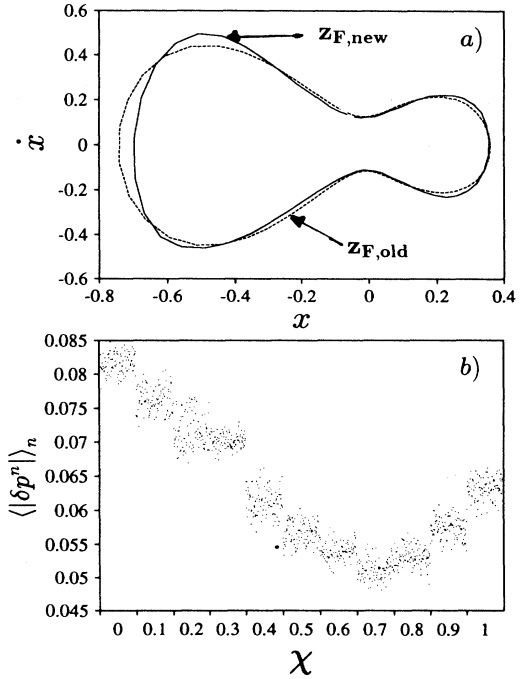

FIG. 2. (a) In the x-$\dot{x}$ plane, $\hat{\mathbf{z}}_{F,\text{old}}^n$, used as $\mathbf{z}_F^n$ in the feedback control, and the corrected orbit $\hat{\mathbf{z}}_{F,\text{new}}^n$ are shown. (b) The old value $\mathbf{z}_{F,\text{old}}^n$ is not immediately replaced by $\hat{\mathbf{z}}_{F,\text{new}}^n$ in the feedback loop. Instead the weighted average $\mathbf{z}_F^n(\chi) = (1-\chi)\,\mathbf{z}_{F,\text{old}}^n + \chi\,\mathbf{z}_{F,\text{new}}^n$ is used for the local control beginning with $\chi = 0$ and increasing χ after 100 driving periods by 0.1. Depending on the weighting factor χ, the magnitude of the averaged control signal $\langle |\delta p^n| \rangle_n$ varies. As optimal χ we take the one that minimizes the averaged control signal, here $\chi_{\text{opt}} = 0.7$.

TRACKING THE BRONZE RIBBON

Now that we can systematically improve the estimate of the true orbit $\hat{\mathbf{z}}_F^n$ during control we have the crucial prerequisite at hand for tracking an UPO. Although in principle it is necessary in a tracking process to adapt besides $\mathbf{z}_F^n(p)$ also the control vector $\mathbf{K}^n(p)$, we neglected this point in a first attempt to track an UPO of the experimental bronze ribbon. For the starting parameter $p = 0$ V we determined the control values $\mathbf{z}_F^n(p = 0\text{ V})$, $A^n(p = 0\text{ V})$, $\mathbf{w}^n(p = 0\text{ V})$, and $\mathbf{K}^n(p = 0\text{ V})$ using the

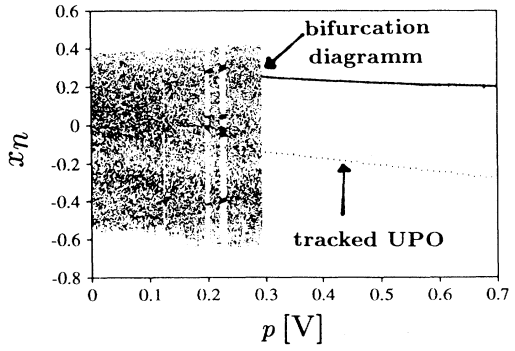

FIG. 3. Bifurcation diagram of the bronze ribbon for the tracking regime $p = 0$ V $-$ 0.7 V. Note that for $p = 0.7$ V the offset of the voltage exceeds the amplitude $U_A = 0.6$ V of the sinusoidal driving (see Fig. 1). In addition, the tracked orbit is plotted in the diagram. As the size of the tracking steps we used $\Delta p = 0.01$ V.

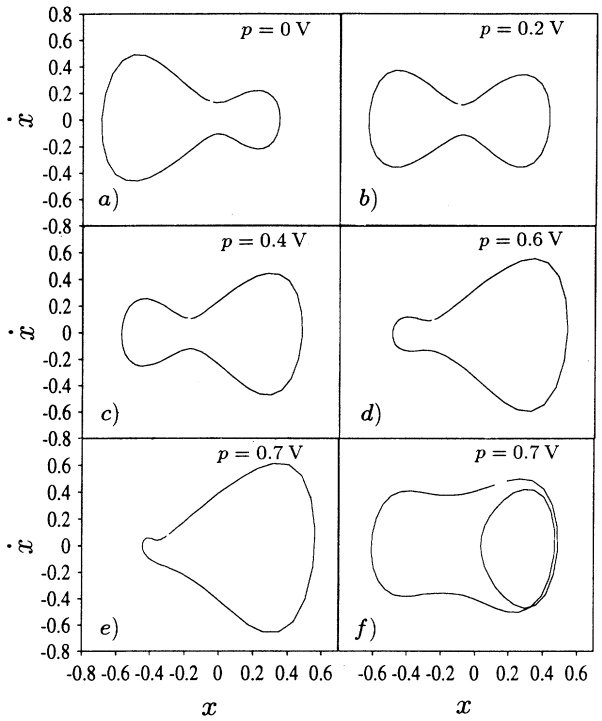

FIG. 4. Tracked UPO for different parameters p along the tracking process in the x-$\dot{x}$ plane. We start to draw the curve at $(x, \dot{x})$ values corresponding to the Poincaré section $t = 0$. In (e) we have, for comparison, plotted the coexisting stable orbit at $p = 0.7$ V.

method of best recurrent points, linear fits in embedding space, and the shift of the UPO for a slight change of the parameter p [11]. After the stabilization of the corresponding UPO the tracking process is started, using as the size of the tracking step $\Delta p = 0.01$ V. For each tracking step the value of $\mathbf{z}_F^n(p + \Delta p)$ is calculated using repeated orbit correction combined with a reduction of $\delta p_{\max}$. Before starting the next tracking step, the resulting value of $\delta p_{\max}$ is set to $1.5\,\delta p_{\max}$ in order not to lose the UPO in the next tracking step.

We succeed to track the UPO from $p = 0$ V to $p = 0.7$ V using an averaged control signal of no more than 0.05 V. In Fig. 3 the bifurcation diagram with the tracked UPO included reveals that we are able to track the UPO into a parameter regime where the system has switched to a stable period-one behavior. In Fig. 4 the continuous change of the tracked UPO can be seen. The final UPO at $p = 0.7$ V [Fig. 4(e)] differs drastically from the coexisting stable orbit [Fig. 4(f)].

The successful tracking is a little bit surprising if one remembers that we did not redetermine the control vector $\mathbf{K}^n(p)$ for the feedback and $A^n(p)$ and $\mathbf{w}^n(p)$, which crucially enter formula (7) for the orbit correction. A possible reason for the success is that for the UPO considered in the experiment these quantities do not change drastically. This has been seen by determining A^n and $\mathbf{w}^n$ for different p. But to apply the tracking method with the adaptive orbit correction of Doerner to general systems, a redetermination of A^n and $\mathbf{w}^n$ during control should be tried. One possible approach could be to fit A^n and $\mathbf{w}^n$ using the observed $\delta\mathbf{z}^n$ and δp^n of the controlled system together with Eq. (4). Another field of future work will be the tracking of higher periodic orbits which we have not attempted yet.

To summarize, we successfully tracked unstable periodic-one orbits of a mechanical experiment. Starting with feedback control vectors extracted from scalar measurement data at each tracking step, the new position of the UPO is redetermined using the adaptive orbit correction, which exploits during control the control signal and the actual behavior of the system. As the adaptive orbit correction reduces the necessary control signal, the local control itself becomes more robust against external disturbances. In the tracking process we are able to track the orbit over a broad parameter regime entering parameter regions where the chaotic attractor has disappeared and another periodic orbit has become stable.

[1] E. Ott, C. Grebogi, and J.A. Yorke, Phys. Rev. Lett. **64**, 1196 (1990).
[2] T. Shinbrot, C. Grebogi, E. Ott, and J.A. Yorke, Nature **363**, 411 (1993).
[3] I.B. Schwartz and I. Triandaf, Phys. Rev. A **46**, 7439 (1992).
[4] Z. Gills, C. Iwata, R. Roy, I.B. Schwartz, and I. Triandaf, Phys. Rev. Lett. **69**, 3169 (1992).
[5] T.L. Carroll, I. Triandaf, I.B. Schwartz, and L. Pecora, Phys. Rev. A **46**, 6189 (1992).
[6] V. Petrov, M.J. Crowley, and K. Showalter, Phys. Rev. Lett. **72**, 2955 (1994).
[7] S. Bielawski, D. Derozier, and P. Glorieux, Phys. Rev. A **47**, R2492 (1993).
[8] E.R. Hunt, Phys. Rev. Lett. **67**, 1953 (1991).
[9] F.J. Romeiras, C. Grebogi, E. Ott, and W.P. Dayawansa, Physica D **58**, 165 (1992).
[10] R. Doerner, B. Hübinger, and W. Martienssen (unpublished).
[11] B. Hübinger, R. Doerner, W. Martienssen, M. Herdering, R. Pitka, and U. Dressler, Phys. Rev. E **50**, 932 (1994).
[12] B. Hübinger, R. Doerner, and W. Martienssen, Z. Phys. B **90**, 103 (1993).
[13] F.C. Moon, *Chaotic Vibrations* (Wiley, New York, 1987).